THE JOURNAL OF PHYSICAL CHEMISTRY B LETTERS

2005, *109,* 13403−13405
Published on Web 06/24/2005

Magnetic Properties of Monodispersed Ni/NiO Core−Shell Nanoparticles

Takafumi Seto,*,† Hiroyuki Akinaga,‡ Fumiyoshi Takano,‡ Kenji Koga,‡ Takaaki Orii,† and Makoto Hirasawa†

Research Consortium for Synthetic Nano-Function Materials Project (SYNAF), National Institute of Advanced Industrial Science and Technology (AIST), Central 2, 1-1-1 Umezono, Tsukuba, Ibaraki 305-8568, Japan

Received: April 22, 2005; In Final Form: June 16, 2005

We have recently developed a method to fabricate monodispersed Ni/NiO core−shell nanoparticles by pulsed laser ablation (Sakiyama, et al. *J. Phys. Chem. B* **2004**, *108*, 523). In this report, the size-dependent magnetic properties of monodispersed Ni/NiO core−shell nanoparticles were investigated. These nanoparticles were formed in two steps. The first was to fabricate a series of monodispersed Ni nanoparticles of 5 to 20 nm in diameter using a combination of laser ablation and size classification by a low-pressure differential mobility analyzer (DMA). The second step was to oxidize the surfaces of the Ni particles in situ to form core−shell structures. A superconducting quantum interference device (SQUID) magnetometer was used to measure the magnetic properties of nanostructured films prepared by depositing the nanoparticles at room temperature. Ferromagnetism was observed in the magnetic hysteresis loop of the nanostructured films composed of core−shell nanoparticles with core diameters smaller than the superparamagnetic limit, which suggests the spin of Ni core was weakly exchange coupled with antiferromagnetic NiO shell. In contrast, smaller nanoparticles with core diameters of 3.0 nm exhibited superparamagnetism. The drastic change in the hysteresis loops between field-deposited and zero-field-deposited samples was attributable to the strong anisotropy that developed during the magnetic-field-assisted nanostructuring process.

Introduction

Nanometer-sized transient metal particles exhibit a variety of unique magnetic properties.[1] The magnetization in single-domain nanoparticles occurs via spins rotation (magnetization reversal mode), while nanoparticles below a critical size manifest superparamagnetism (SPM)[2] due to a competition between the thermal fluctuation of spin and the ordering. This critical size results in a "superparamagnetic limit" in the application of nanoparticles to ultrahigh-density magnetic recording media. One method to surmount this limit is to apply a newly developed series of highly anisotropic magnetic nanoparticles such as fct FePt and CoPt, together with their superlattice array.[3] Alternatively, the exchange coupling at the interface between ferromagnetic (FM) and antiferromagnetic (AFM) substances cooled under a magnetic field can be used to generate large coercivity and hysteresis loop shift, a phenomenon referred to as "exchange bias".[4] As it turns out, this type of interface can be realized fairly easily in a metallic nanoparticle covered with a metal oxide surface layer, i.e., a core−shell structure. Several groups have enhanced the coercivity with exchange bias in core−shell Co/CoO nanoparticles.[5,6] The key factor in controlling the magnetic interaction of these core−shell nanoparticles is to control the size of the metallic core, the thickness of the metal oxide shell, and the shape, crystallinity, and structure of their array. When applying the exchange bias concept to a nanomagnet or high-density magnetic recoding media that operates at room temperature, care should be taken to choose a material system with a reasonable critical temperature (Neel or Curie temperature). The nickel and nickel oxide system is an attractive option since temperature differential between the Neel temperatures of NiO and CoO (523−647 K vs 293 K) makes it possible to generate exchange coupling at room temperature.[7] On another promising note, remarkably large coercive forces have also been reported in surface-oxidized Ni nanoparticles[8] and in a reduced-sized AFM NiO nanoparticle system.[9,10] Significant technological impacts can thus be expected if researchers succeed in fabricating a morphology-controlled core−shell nanoparticle of Ni/NiO and controlling its anisotropy at room temperature.

Laser ablation is a powerful tool for fabricating high-purity ferromagnetic metal nanoparticles.[11] We recently succeeded in fabricating morphology-controlled Ni/NiO core shell nanoparticles by combining laser ablation and aerosol techniques.[12] In this paper we investigate the size-dependent magnetic properties of these core−shell nanoparticles and discuss our attempts to control the magnetic anisotropy of the nanoparticles at room temperature.

Experimental Section

The monodispersed Ni/NiO core shell nanoparticles were synthesized by (i) pulsed laser ablation (PLA) of a solid target

* Corresponding author.
† Also at: Advanced Manufacturing Research Institute, National Institute of Advanced Industrial Science and Technology (AIST), 1-2-1 Namiki, Tsukuba 305-8564, Japan.
‡ Also at: Nanotechnology Research Institute, National Institute of Advanced Industrial Science and Technology (AIST), AIST Central 5, 1-1-1 Higashi, Tsukuba 305-8565, Japan.

10.1021/jp052084+ CCC: $30.25

TABLE 1: Average Dimensions and Magnetic Coercivity of Core−Shell Nanoparticles

DMA diameter [nm]	core diameter [nm]	shell thickness [nm]	coercivity [Oe]
5	3.0	1.7	0
10	6.2	2.4	10
15	12.8	2.1	15
20	17.4	2.1	30
17.4	[a]		10
20[b]	17.4	2.1	100[c]

[a] The particles were deposited without oxidation. [b] The particles were oxidized/deposited under the magnetic field. [c] No shift in hysteresis was measured.

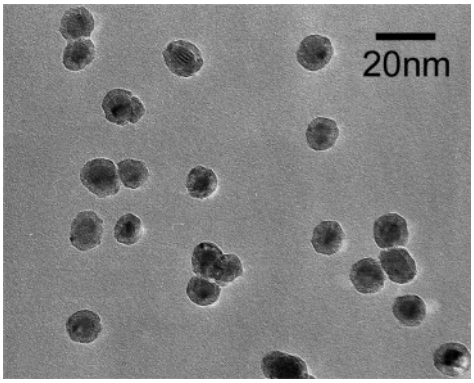

Figure 1. Transmission electron micrograph of Ni/NiO core−shell nanoparticles assigned a mobility-equivalent diameter of 10 nm.

(Ni rod) under 1000 Pa of helium gas, (ii) transport as aerosol and annealing in a gas flow (aerosol post annealing; APA), (iii) size classification by a differential mobility analyzer (DMA), (iv) surface oxidization by mixing the particles with oxygen, and (v) deposition on a substrate. The details of this fabrication technique are described elsewhere.[12] Using this system, we generated core−shell nanoparticles of four sizes (5, 10, 15, and 20 nm) in a mobility equivalent diameter (DMA diameter), as listed in Table 1. During oxidation, the diameters of the Ni cores were reduced to 3.0, 6.2, 12.8, and 17.4 nm, respectively. The thicknesses of the NiO shells were constant at about 2 nm, regardless of the particle size. As a result, the total diameters (core diameter + double the shell thickness) were 1 to 2 nm larger than the DMA diameters. Figure 1 shows a typical transmission electron micrograph of generated Ni/NiO core−shell nanoparticles classified at 10 nm. The particles were single crystals and quite thoroughly monodispersed by the DMA classification (geometric standard deviations less than 1.2).

As each nanoparticle has a single charge, we could roughly measure the amount of nanoparticles deposited on the substrate by measuring their electric current.[13] The substrate was a low-conductivity Si plate (6 × 12 mm), and the diamagnetic background of the Si substrate was subtracted in the hysteresis curves. To control anisotropic interaction at room temperature, we positioned a magnet (0.5 T) under the substrate during nanoparticle deposition is some of our experiments, as mentioned later in this paper.

The nanostructured films formed from the monodispersed core−shell nanoparticles were chemically stable against ambient air since the NiO shell structure protected the Ni core from further oxidation. The magnetic hysteresis curves of the nanostructured films were measured at room temperature using a superconducting quantum interference device (SQUID) magnetometer.

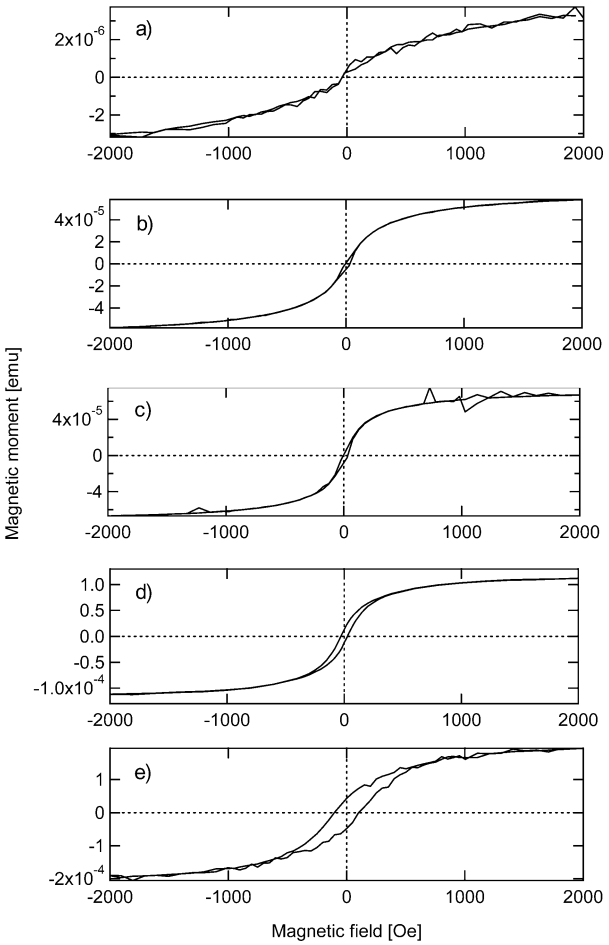

Figure 2. Hysteresis curves measured by SQUID magnetometer. (a) 5 nm, (b) 10 nm, (c) 15 nm, and (d) 20 nm in mobility (DMA) diameters, respectively. (e) The nanoparticles were oxidized and deposited under the magnetic field under the conditions illustrated in Figure 3.

Results and Discussion

Figures 2a−d show the size-dependent hysteresis curves measured at room temperature. The particles with DMA diameters of 20, 15, and 10 nm exhibited ferromagnetism with small coercive forces and saturation moments at a magnetic field of about 1 kOe. The slope of the curve decreased as the size decreased. At the mobility diameter of 5 nm, the curve does not exhibit hysteresis any more and the magnetic moment changed almost linearly with applied magnetic field due to the onset of superparamagnetism (SPM). The critical diameter for SPM, d_c, was calculated as about 35 nm from the formula, $KV = 25kT$, where K is the magnetic anisotropy constant (about 4×10^5 J/m^3 for bulk Ni), V is the particle volume, k is the Boltzmann constant, and T is temperature. In experimental observation, d_c was measured at 15 nm at a coercive force of almost zero.[14] On the other hand, the particles with core a diameter of 6.2 nm in the present study still exhibited ferromagnetic properties with saturation moment, which suggests that NiO shells are successfully isolating each Ni core and the exchange interaction at the Ni/NiO interface plays a role to fix a spin of Ni core. This phenomenon can be confirmed when the Ni nanoparticles of 17.4 nm in mobility diameter were deposited without oxidation. As shown in Table 1, the coercivity (10 Oe) was lower than that of the particles of the same core diameter with NiO shell (it was close to that of 10-nm particles of Ni/NiO). Also, we observed exchange bias of 80 Oe when the magnetometer was operated under the temperature of 5 K.

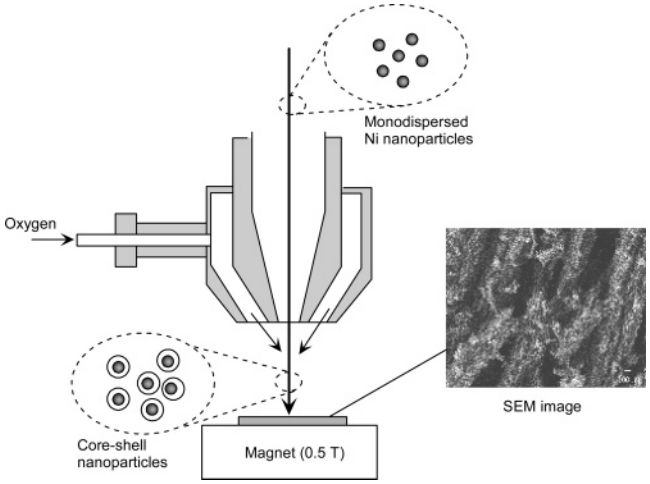

Figure 3. The aerosol deposition system under the magnetic field. Single crystallized and size-selected Ni particles were ejected from the center of the nozzle. The surface of the Ni was oxidized by mixing the particles with oxygen and impacting them on the substrate (Si). The magnet was positioned to apply the magnetic field during the oxidation and the deposition. The scanning electron micrograph shows the aligned structure of Ni/NiO nanoparticles (20 nm in mobility diameter) prepared by the deposition under the magnetic field.

Some researchers have demonstrated a magnetization of finite-sized NiO under low temperature due to a breaking of the oxygen bond and uncompensated spin at the surface.[10] In our case, the AFM NiO shell did not contribute observably in the hysteresis curves at room temperature, and an absence of distinguishable shifts in the hysteresis loops indicated that the exchange anisotropy was not large as well. Although we were unable to quantify the contribution of the NiO shell on the magnetic properties of the Ni core, we could tune the magnetic property of Ni cores by the size-classification and we also conjecture that the spin of Ni core was weakly exchange coupled with AFM NiO shell at the interface. The coercivity, H_c gradually increased with the particle diameter, but it still remained lower than bulk Ni (about 100 Oe), even at the largest particle diameter of 20 nm (see Table 1). Figure 2e shows the change in the hysteresis loop for 20 nm particles deposited under a magnetic field perpendicular to the substrate. Figure 3 illustrates the position of the magnet (0.5 T) used to apply magnetic field during the oxidation and deposition. The hysteresis curve changed remarkably at room temperature. The coercivity, H_c, rose to a value close to that of the bulk Ni when the magnetic field was applied during particle structuring. We were also interested to note an absence of shift in the hysteresis loop, an indication that the exchange anisotropy was somewhat small in the present Ni−NiO system, as previously reported by Sako et al.[15] Moreover, the slope in the hysteresis curve was reduced. It therefore appeared that the easy axes of the Ni cores were aligned to one direction (perpendicular to the substrate) during the nanostructuring process under the magnetic field and that the NiO shells were pinning the spin of the interface, as mentioned before. As a result, the energy barrier and magnetic anisotropy were formed perpendicularly to the substrate, and thereby increased the coercive force against the magnetic field oriented horizontally to the substrate during SQUID measurements. Such alignment of Ni/NiO nanoparticles was sometimes observed when the magnetic field was applied during the deposition process as shown in the scanning electron micrograph (Figure 3). The particles were one-dimensionally aligned to the direction of magnetic field. We also observed the change in the hysteresis curve depending on the orientation of the sample in the magnetometer.

Conclusions

In summary, our group observed the changes in the magnetic properties of Ni/NiO core−shell nanoparticles of different sizes both with and without the application of a magnetic field during nanostructuring. The smallest-diameter particles measuring 3 nm exhibited a reduction of the slope in the hysteresis curve due to superparamagnetism. The larger particles of 6.2, 12.8, and 17.4 nm in core diameters exhibited dominant ferromagnetism due to the weak exchange coupled spin at the Ni/NiO interface. We managed to drastically alter both the coercivity and hysteresis by imposing a one-dimensional alignment of the spin in conjunction with pinning by the AFM shell. While further data on thermal activation and the spin structure will certainly be needed, we have successfully demonstrated a method to control the magnetic property of Ni/NiO core−shell nanoparticles.

Acknowledgment. This study was supported in part by the New Energy and Industrial Technology Development Organization (NEDO) under the Nanotechnology Materials Program.

Supporting Information Available: Hysteresis curves for Ni without NiO shell, for Ni/NiO measured at 5K, and for Ni/NiO measured in different orientation are enclosed in the Supporting Information. This material is available free of charge via the Internet at http://pubs.acs.org.

References and Notes

(1) Kodama, R. H. *J. Magn. Magn. Mater.* **1999**, *200*, 359−372.
(2) Frei, E. H.; Shtrikman, S.; Treves, D. *Phys. Rev.* **1957**, *106*, 446.
(3) Sun, S. H.; Murray, C. B.; Weller, D.; Folks, L.; Moser, A. *Science* **2000**, *287*, 1989.
(4) Berkowitz, A. E.; Takano, K. *J. Magn. Magn. Mater.* **1999**, *200*, 552.
(5) Meiklejohn, W. H.; Bean, C. P. *Phys. Rev.* **1956**, *102*, 1413.
(6) Peng, D. L.; Sumiyama, K.; Hihara, T.; Yamamoto, S.; Konno, T. J. *Phys. Rev. B* **2000**, *61*, 3103.
(7) Fraune, M.; Rudiger, U.; Guntherodt, G.; Cardoso, S.; Freitas, P. *Appl. Phys. Lett.* **2000**, *77*, 3815.
(8) Sun, X. C.; Dong, X. L. *Mater. Res. Bull.* **2002**, *37*, 991.
(9) Kodama, R. H.; Marklouf, S. A.; Berkowitz, A. E. *Phys. Rev. Lett.* **1997**, *79*, 1393.
(10) Makhlouf, S. A.; Parker, F. T.; Spada, F. E.; Berkowitz, A. E. *J. Appl. Phys.* **1997**, *81*, 5561.
(11) Jonsson, B. J.; Turkki, T.; Strom, V.; El-Shall, M. S.; Rao, K. V. *J. Appl. Phys.* **1996**, *79*, 5063.
(12) Sakiyama, K.; Koga, K.; Seto, T.; Hirasawa, M.; Orii, T. *J. Phys. Chem. B* **2004**, *108*, 523.
(13) Seto, T.; Koga, K.; Akinaga, H.; Takano, F.; Orii, T.; Hirasawa, M. *Appl. Phys. A* **2004**, *79*, 1165.
(14) Du, Y. W.; Xu, M. X.; Shi, Y. B.; Lu, H. X. *J. Appl. Phys.* **1991**, *70*, 5903.
(15) Sako, S.; Ohshima, K.; Sakai, M.; Bandow, S. *J. Vac. Sci. Technol. B* **1997**, *15*, 1338.